5 November 1999

ELSEVIER

Chemical Physics Letters 313 (1999) 171–178

CHEMICAL PHYSICS LETTERS

www.elsevier.nl/locate/cplett

Rotationally resolved electronic absorption spectra of triacetylene cation in a supersonic jet

David Pfluger, Wayne E. Sinclair *, Harold Linnartz, John P. Maier

Institute for Physical Chemistry, University of Basel, Klingelbergstrasse 80, CH-4056 Basel, Switzerland

Received 30 July 1999; in final form 27 August 1999

Abstract

The rotationally resolved cold spectra ($T_{rot} \approx 17$ K) of the $A\,^2\Pi_g \leftarrow X\,^2\Pi_u$ 0_0^0 and 4_0^1 transitions of triacetylene cation have been recorded in a supersonic jet. A discharge modulation in combination with the external frequency modulation of a cw ring laser is used to enhance detection sensitivity. The advantage of obtaining the spectra of such species under jet conditions is shown by comparison with measurements in a cell of the 4_0^1 vibronic transition. The combined analyses of the rotational structure yields rotational and spin–orbit constants for the $\nu_4 = 1$ level of the $A\,^2\Pi_g$ state.

1. Introduction

Optical frequency modulation (FM) absorption spectroscopy is an established technique based on the method of heterodyne spectroscopy. The technique utilizes an external phase modulator to produce wavelength modulation and has proven to be a sensitive absorption method to detect stable molecules [1–3] as well as transient species [4]. Discharge modulation coupled with phase sensitive detection is commonly adopted to achieve a high degree of sensitivity and selectivity in the spectroscopic characterization of transient species. A combination of these techniques has been used to observe the origin band of the $A\,^2\Pi \leftarrow X\,^2\Pi$ electronic transition of polyacetylene [5] and cyanopolyacetylene [6] cations generated in a hollow-cathode discharge cell with Doppler-limited resolution.

The high rotational and translational temperatures typical for a discharge cell increase the spectral complexity of $^2\Pi \leftarrow {}^2\Pi$ type spectra and hot bands can have significant intensity, adding to the spectral congestion. This can be overcome by cooling in a free jet expansion. The effective production of carbon chains in a pulsed supersonic slit-jet discharge assembly has been demonstrated previously by detection in direct absorption using cavity ring down spectroscopy [7]. The technique of transient FM absorption spectroscopy has been successfully developed to detect free radicals in pin hole and slit supersonic jets [8], while discharge modulation combined with a pulsed expansion has been used for phase sensitive detection of transient species with improved signal to noise [9].

* Corresponding author. Fax: +41-61-267-3855; e-mail: sinclair@ubaclu.unibas.ch

0009-2614/99/$ - see front matter
PII: S0009-2614(99)00984-7

In the present work, a FM technique has been applied for the sensitive detection of triacetylene (HC_6H^+) cation generated in a pulsed slit-jet discharge. The characteristics of the method are illustrated by recording the rotationally resolved cold spectra of the $A^2\Pi_g \leftarrow X^2\Pi_u$ origin band of HC_6H^+. The advantage of obtaining both cell and jet spectra is demonstrated for the $A^2\Pi_g \leftarrow X^2\Pi_u\ 4_0^1$ transition of HC_6H^+, where ν_4 is the totally symmetric C–C stretch. The combined analyses of the fully resolved rotational structure yield the first accurate values of the rotational constants and spin–orbit constants for the $\nu_4 = 1$ level of the $A^2\Pi_g$ state.

2. Experimental

Fig. 1 shows the experimental setup. The slit nozzle/electrode assembly was similar to that described [10]. The cathode consisted of two stainless-steel jaws that form the slit (30 mm × 200 μm). The anode was a 1 mm thick metal plate electrically insulated from the cathode by a 1 mm ceramic spacer. The electrode assembly was mounted via a 1.5 mm ceramic spacer to a floating metal body by electrically insulated screws. The body was fixed to a pulsed valve with a 2 mm circular orifice. The nozzle was mounted in a Perry type multi-pass system ($L = 300$ mm) inside the vacuum chamber. An effective path length of 39 cm was achieved with 13 passes crossing near the expansion center plane. A roots pump backed by a double-stage rotary pump was used to evacuate the chamber and to maintain a background pressure below 10^{-3} mbar.

The plasma is generated by applying a rectified pulsed ac voltage to the cathode. The ac voltage was driven by a sine-wave generator chopped with an analog switch synchronized with the gas pulse, amplified and stepped up by a transformer, typically to −500 V. The anode was kept at earth potential. The discharge modulation frequency was limited by the

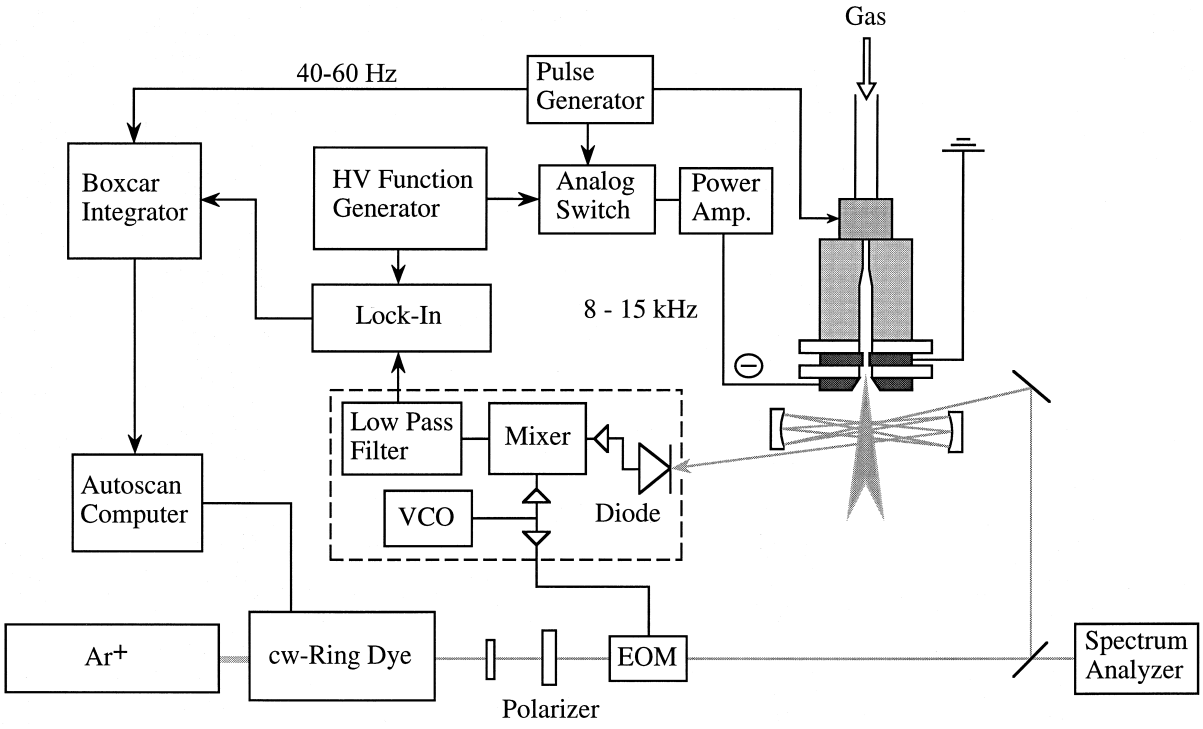

Fig. 1. Schematic diagram of the experimental apparatus used to record FM absorption spectra of HC_6H^+ in a slit-jet discharge.

time the molecules take to cross the detection region, giving an upper limit of ~20 kHz. However, in this case, the optimum signal was obtained with a discharge modulation at 8 kHz. The HC_6H^+ ion was generated by introducing a gas mixture of 0.3% C_2H_2 diluted in He or Ar gas. Typically, a backing pressure of 7–10 bar with a gas pulse of ~1 ms duration was used at a repetition rate of 40–60 Hz. During jet operation the pressure in the chamber was ~0.6–0.9 mbar.

The experimental approach used for absorption measurements of transient species by a combination of FM and discharge modulation has also been described [5]. A single-mode ring dye laser pumped by an 8 W cw Ar^+ laser was phase-modulated at a radio frequency of 192 MHz by an electro-optic modulator (EOM). Radio frequency power into the modulator was adjusted to give first-order sidebands typically 25% of the carrier frequency intensity as monitored by a Fabry–Pérot étalon spectral analyzer. The frequency-modulated laser beam was aligned through the chamber, ~5 mm from the slit nozzle orifice. The high-frequency components of the photodiode were amplified and demodulated in a double-balanced mixer, referenced to the local radio frequency source, which drives the EOM. The signal was fed to a lock-in amplifier to extract the signal at the discharge modulation frequency with a time constant of 1 ms. The output of the lock-in was then fed to a boxcar integrator, using the reference signal from the pulsed valve (40–60 Hz), and interfaced to a PC with autoscan system software for data collection.

Absolute frequency calibration was performed by simultaneously recording the I_2 absorption spectrum with an estimated accuracy of better than 0.005 cm^{-1}. The instrumental lineshape is approximately first derivative due to the modulation scheme employed. The rotationally resolved spectra were analyzed using the simulation and least-squares fitting program Pgopher [11].

3. Results and discussion

The high-resolution $A^2\Pi_g \leftarrow X^2\Pi_u$ origin band of HC_6H^+ recorded in the slit-jet discharge is shown

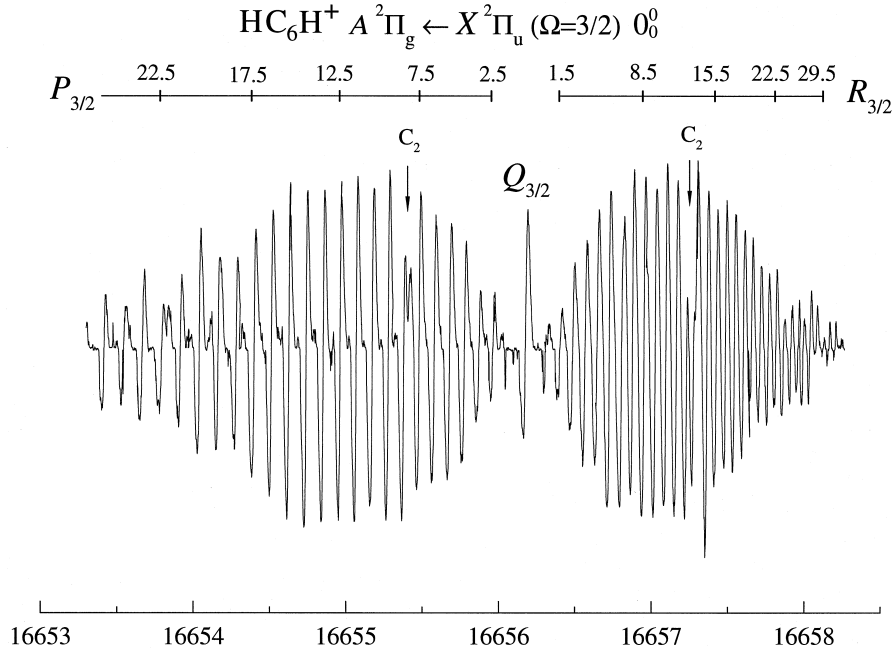

Fig. 2. Rotationally resolved FM absorption spectrum of the $A^2\Pi_g \leftarrow X^2\Pi_u$ ($\Omega = 3/2$) 0_0^0 band of HC_6H^+ recorded with a slit-jet discharge expansion of C_2H_2 with He as carrier gas. The rotational assignments are given at the top of the each spectrum. Minor disturbances due to C_2 transitions are indicated.

Table 1
Frequencies (in cm^{-1}) and assignments for the $A^2\Pi_g \leftarrow X^2\Pi_u$ 4_0^1 absorption spectrum of $C_6H_2^+$ and residuals from the fit

J	obs.	o−c[a]	J	obs.	o−c[a]	J	obs.	o−c[a]	J	obs.	o−c[a]	J	obs.	o−c[a]	J	obs.	o−c[a]
$R_{3/2}(J)$			$P_{3/2}(J)$						$R_{1/2}(J)$			$P_{1/2}(J)$					
1.5	17274.343	3	2.5	17273.900	1	42.5	17268.885	2	0.5			1.5			41.5		
2.5	17274.423	−1	3.5	17273.801	−5	43.5	17268.724	0	1.5			2.5			42.5	17265.628	1
3.5	17274.505	0	4.5	17273.716	5	44.5	17268.567	3	2.5			3.5			43.5	17265.468	−1
4.5	17274.590	5	5.5	17273.617	2	45.5	17268.403	3	3.5			4.5	17270.452	2	44.5	17265.310	2
5.5	17274.666	2	6.5	17273.516	−1	46.5	17268.237	1	4.5			5.5			45.5	17265.144	−2
6.5	17274.743	3	7.5	17273.413	−3	47.5	17268.075	5	5.5	17271.406		6.5			46.5	17264.988	−6
7.5	17274.816	1	8.5	17273.312	−3	48.5	17267.904	2	6.5			7.5	17270.155	0	47.5	17264.812	−5
8.5	17274.887	−2	9.5	17273.212	0	49.5	17267.735	2	7.5			8.5	17270.054	1	48.5	17264.651	1
9.5	17274.962	2	10.5	17273.104	−4	50.5	17267.555	−7	8.5	17271.630	−1	9.5			49.5	17264.479	−2
10.5	17275.029	−1	11.5	17272.998	−3	51.5	17267.392	3	9.5			10.5	17269.842	−3	50.5	17264.312	1
11.5	17275.098	−1	12.5	17272.892	−1	52.5	17267.214	−1	10.5	17271.777	3	11.5	17269.738	−1	51.5	17264.136	−3
12.5	17275.167	1	13.5	17272.781	0	53.5	17267.039	0	11.5	17271.845	2	12.5			52.5	17263.968	−3
13.5	17275.232	1	14.5	17272.675	3	54.5	17266.857	−5	12.5	17271.910	0	13.5			53.5	17263.789	−1
14.5	17275.294	0	15.5	17272.559	0	55.5	17266.684	2	13.5			14.5	17269.409	−1	54.5	17263.617	4
15.5	17275.356	0	16.5	17272.444	0	56.5	17266.503	1	14.5	17272.042	2	15.5	17269.296	−1	55.5	17263.433	−2
16.5	17275.415	−1	17.5	17272.328	0	57.5	17266.319	0	15.5			16.5			56.5	17263.260	6
17.5	17275.473	−2	18.5	17272.212	2	58.5	17266.134	−1	16.5	17272.162	−1	17.5	17269.069	3	57.5	17263.070	−3
18.5	17275.532	1	19.5	17272.093	3	59.5	17265.946	−3	17.5			18.5	17268.951	3			
19.5	17275.587	0	20.5	17271.967	−2	60.5	17265.758	−3	18.5	17272.281	2	19.5	17268.832	4			

20.5	17275.641	1	21.5	17271.845	−1	61.5	17265.570	−2	19.5			20.5		
21.5	17275.694	2	22.5	17271.719	−3	62.5	17265.380	−1	20.5	17272.389	0	21.5		
22.5	17275.743	1	23.5	17271.595	−1	63.5	17265.187	−2	21.5	17272.444	2	22.5	17268.463	3
23.5	17275.791	0	24.5	17271.469	1	64.5	17264.990	−4	22.5	17272.494	1	23.5	17268.336	2
24.5	17275.844	6	25.5	17271.333	−5	65.5	17264.812	5	23.5			24.5	17268.207	1
25.5	17275.885	2	26.5	17271.204	−3	66.5	17264.600	−1	24.5	17272.591	2	25.5	17268.072	−5
26.5	17275.930	3	27.5	17271.072	−2	67.5	17264.400	−2	25.5	17272.635	−1	26.5	17267.947	1
27.5	17275.971	2	28.5	17270.938	−2	68.5	17264.202	1	26.5			27.5	17267.814	1
28.5	17276.010	1	29.5	17270.802	−2	69.5	17263.997	−1	27.5	17272.724	2	28.5	17267.683	4
29.5	17276.050	2	30.5	17270.664	−2	70.5	17263.791	−3	28.5			29.5		
30.5	17276.088	3	31.5	17270.527	1	71.5	17263.588	0	29.5			30.5		
31.5	17276.122	2	32.5	17270.387	2	72.5	17263.381	1	30.5	17272.840	−1	31.5	17267.266	0
32.5	17276.152	−2	33.5	17270.246	4	73.5	17263.174	3				32.5	17267.125	−1
33.5	17276.185	−1	34.5	17270.095	−3	74.5	17262.960	0				33.5	17266.982	−1
34.5	17276.216	0	35.5	17269.952	0							34.5		
35.5	17276.242	−3	36.5	17269.803	−1							35.5	17266.688	−5
36.5	17276.269	−3	37.5	17269.654	−1							36.5	17266.549	3
37.5	17276.295	−2	38.5	17269.509	5							37.5	17266.393	−4
			39.5	17269.348	−3							38.5	17266.246	0
$Q_{3/2}(J)$			40.5	17269.194	−3							39.5	17266.092	−2
1.5	17274.113	−2	41.5	17269.042	1							40.5	17265.941	1

[a](o − c) in units of 10^{-3} cm^{-1}.

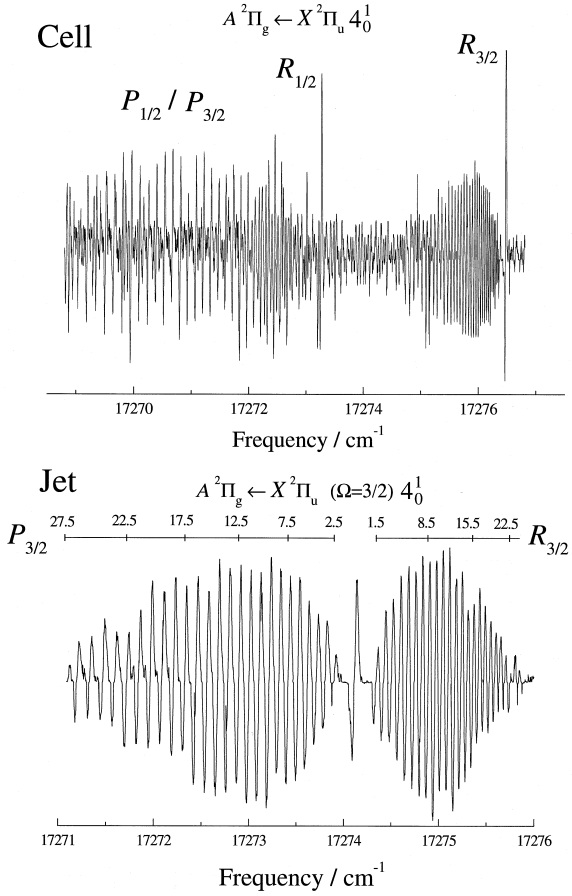

Fig. 3. Rotationally resolved FM absorption spectrum of the $A\,^2\Pi_g \leftarrow X\,^2\Pi_u$ 4_0^1 band of HC_6H^+ recorded with a liquid-nitrogen-cooled hollow-cathode (upper trace) and slit-jet (lower trace) discharges of a C_2H_2/He mixture.

in Fig. 2. The 0_0^0 band was the subject of previous investigations in a hollow-cathode discharge cell [5]. At the high ambient temperature of the cell (170 K), it was found to comprise of two sub-bands attributed to the $\Omega = 1/2$ and $\Omega = 3/2$ components separated by the difference in the spin–orbit interaction constant for each electronic state, $|A_0'' - A_0'|$. The sub-bands comprised strong P and R branches and a relatively weak Q branch. As the electronic states are well described by the configurations $\ldots 1\pi_g^4 2\pi_u^3$ $X\,^2\Pi_u$ and $\ldots 1\pi_g^3 2\pi_u^4$ $A\,^2\Pi_g$, the $\Omega = 3/2$ component is expected to be lower lying than $\Omega = 1/2$ (inverted sequence) with the spin–orbit constant having a negative value.

In contrast to the recording in a discharge cell, the jet spectrum displays a single band. It consists of a well-defined P and R branch. Most significant is the appearance of a prominent Q branch. In addition, the lower J transitions are markedly stronger in the jet spectrum and no band head is observed in the R branch. The band exhibits a band gap of $\sim 10\,B$, establishing that the first transitions in the P and R branches are P(2.5) and R(1.5) and that it corresponds to that of the $\Omega = 3/2$ component.

These observations are consistent with the low rotational temperature attained in the supersonic jet. The band was reproduced using the rotational constants derived previously [5]. From the relative intensity of the P and R branches, the rotational temperature is estimated as 15–20 K. The lower temperature favors the population of the low-J rotational levels. For electronic transitions with $\Delta\Lambda = 0$, the Q-line strength S_{JJ} is given by $S_{JJ} = \Omega^2(2J+1)/[J(J+1)]$ and is expected to be of significant intensity at low temperatures. The spin–orbit splitting of HC_6H^+ in the $X\,^2\Pi_u$ state is ~ -31 cm^{-1} [5]. Therefore, the population of the $\Omega = 1/2$ component is moderate at such low temperatures and indeed the $\Omega = 1/2$ sub-band was not detected. This feature allowed the observation of a number of rotational lines that were overlapped and obscured by the $\Omega = 1/2$ component

Table 2
Molecular constants (in cm^{-1}) of HC_6H^+ in the $X\,^2\Pi_u$ $v = 0$ and $A\,^2\Pi_g$ $v = 0$, $v_4 = 1$ states, derived from analysis of the rotationally resolved absorption spectra. N is the number of lines used in the fit; $o - c$ is the observed minus calculated standard deviation of the fit[a]

	$X\,^2\Pi_u$ state	
	$v_4 = 0$	$v_0 = 0$[b]
B_0''	0.044613 (11)	0.0445943 (34)
A_0''	−32.81 (80)	−31.40 (28)
	$A\,^2\Pi_g$ state	
	$v_4 = 1$	$v_0 = 0$[b]
B_0'	0.043792 (11)	0.0437921 (34)
ΔA	−3.257	−2.993
ν_0	17272.49470 (37)	16654.68726 (25)
N	169	277
o − c	0.0025	0.0024

[a] One standard deviation given in parentheses.
[b] Ref. [5].

in the cell spectra at 170 K. The numbering of the rotational lines is indicated in Fig. 2.

Each rotational linewidth (FWHM) is ~ 650 MHz. Assuming a Doppler-broadened HC_6H^+ signal, this would correspond to a translational temperature of ~ 270 K. This is much higher than obtained in the discharge cell (~ 170 K) and suggests additional contributions to the linewidth that are due to He as a carrier gas. The use of the slower Ar gas resulted in a reduction in the rotational linewidth to ~ 400 MHz and seems to confirm that Doppler broadening is involved. The signal to noise of the strongest transitions in the jet is comparable to that obtained in the cell spectrum. As the total effective pathlength in the jet is significantly shorter than in the cell configuration, the molecular densities are substantially larger in the slit plasma.

To further demonstrate the sensitivity and advantage of the technique, the FM spectrum of the 4_0^1 ($\Omega = 3/2$) vibronic band at 617 cm^{-1} above the 0_0^0 band of HC_6H^+ was recorded in the cell and jet. According to the laser excitation spectrum of HC_6H^+, the 4_0^1 transition is about a factor of 5 less intense than the 0_0^0 transition [12]. The 4_0^1 transition was recorded in a hollow-cathode discharge cell in the range 17 263–17 274 cm^{-1}. A portion of the spectrum is shown in the upper trace of Fig. 3. It is qualitatively similar in appearance to the cell spectrum of the 0_0^0 transition [5]. Two prominent R band heads are observed towards the blue end of the spectrum. Each band head is associated with one vibronic sub-band comprising strong, well-defined P and R branches extending from a relatively weak Q branch head near the origin. The vibronic sub-bands are attributed to the $\Omega = 1/2$ and $\Omega = 3/2$ spin–orbit components separated by ~ 3 cm^{-1}.

The band center of the $\Omega = 3/2$ component of the 4_0^1 band is congested and thus the $Q_{3/2}$ branch and the $P_{3/2}$ and $R_{3/2}$ branch transitions at low J values are not readily identified. Therefore an unambiguous assignment of the rotational levels directly from the band is prevented. However, the corresponding jet spectrum provides the information. The 4_0^1 ($\Omega = 3/2$) vibronic band is shown in the lower trace of Fig. 3. The clear identification of the first transitions in the $P_{3/2}$ and $R_{3/2}$ branch lead to the unambiguous numbering of the lines at high J values in the cell spectrum.

A total of 169 transitions were assigned in the $A^2\Pi_g \leftarrow X^2\Pi_u$ 4_0^1 band of HC_6H^+. Rotational analysis of the spectra followed standard procedures. The line positions were fit with an effective rotational Hamiltonian where both spin–orbit systems were considered simultaneously. The band origin (ν_0), the rotational constant (B_0), centrifugal distortion constant (D_0) and spin–orbit interaction constant (A_0) of both states were adjustable parameters. The line positions of the observed lines in the 4_0^1 band of HC_6H^+ could be fit to standard deviations that are less than the observed linewidths. The observed line positions and residuals are gathered in Table 1.

The optimal values of the molecular constants are shown in Table 2. The D_0 parameters were on the order of 10^{-9}, but had uncertainties as large as the values obtained and are not shown in Table 2. Note, that the parameters for the $X^2\Pi_u$ state are the same within 2σ, as those derived for the 0_0^0 band, also listed. This shows that the transitions originate in the same level, the $v = 0$ level of the $X^2\Pi_u$ state. The value of ΔA derived for the 4_0^1 band is -3.22 cm^{-1} and is comparable to that found for the 0_0^0 band.

In summary, the present study has demonstrated the successful application of the FM technique to a supersonic jet. The good sensitivity and low rotational temperature achievable makes this a useful method for direct absorption studies of carbon chain molecular ions which generally have complicated spectra at higher temperatures. The observed linewidths are satisfactory for the present work, but will need to be improved to study longer members of these series. The current modulation scheme also allows the discrimination between molecular species with quite different lifetimes. Whereas C_2 and C_3 transitions normally dominate the spectra, these are nearly absent in the jet spectrum by using a production modulation period that is shorter than their lifetime. As the technique works well for carbon discharges, application to less corrosive plasmas should be straightforward.

Acknowledgements

This work was supported by the Swiss National Science Foundation, project number 20-55285.98.

References

[1] G.C. Bjorklund, Opt. Lett. 5 (1980) 15.
[2] G.C. Bjorklund, M.D. Levenson, Phys. Rev. A 24 (1981) 166.
[3] J.L. Hall, L. Hollberg, T. Baer, H.G. Robinson, Appl. Phys. Lett. 39 (1981) 680.
[4] J.C. Bloch, R.W. Field, G.E. Hall, T.J. Sears, J. Chem. Phys. 101 (1994) 1717.
[5] W.E. Sinclair, D. Pfluger, H. Linnartz, J.P. Maier, J. Chem. Phys. 110 (1999) 296.
[6] W.E. Sinclair, D. Pfluger, J.P. Maier, J. Chem. Phys. (in press).
[7] H. Linnartz, T. Motylewski, J.P. Maier, J. Chem. Phys. 109 (1998) 3819.
[8] B.-C. Chang, T.J. Sears, Chem. Phys. Lett. 256 (1996) 288.
[9] M. Ishiguro, T. Imajo, K. Harada, M. Matsubara, K. Tanaka, T. Tanaka, Chem. Phys. Lett. 263 (1996) 629.
[10] T. Motylewski, H. Linnartz, Rev. Sci. Instrum. 70 (1999) 1305.
[11] C.M. Western, School of Chemistry, University of Bristol, Bristol, Pgopher version 3.73, 1994.
[12] D. Klapstein, R. Kuhn, J.P. Maier, M. Ochner, W. Zambach, J. Phys. Chem. 88 (1984) 5176.